nature climate change

LETTERS

PUBLISHED ONLINE: 27 JULY 2015 | DOI: 10.1038/NCLIMATE2736

Increasing risk of compound flooding from storm surge and rainfall for major US cities

Thomas Wahl[1,2]*, Shaleen Jain[3], Jens Bender[2,4], Steven D. Meyers[1] and Mark E. Luther[1]

When storm surge and heavy precipitation co-occur, the potential for flooding in low-lying coastal areas is often much greater than from either in isolation. Knowing the probability of these compound events and understanding the processes driving them is essential to mitigate the associated high-impact risks[1,2]. Here we determine the likelihood of joint occurrence of these two phenomena for the contiguous United States (US) and show that the risk of compound flooding is higher for the Atlantic/Gulf coast relative to the Pacific coast. We also provide evidence that the number of compound events has increased significantly over the past century at many of the major coastal cities. Long-term sea-level rise is the main driver for accelerated flooding along the US coastline[3,4]; however, under otherwise stationary conditions (no trends in individual records), changes in the joint distributions of storm surge and precipitation associated with climate variability and change also augment flood potential. For New York City (NYC)—as an example—the observed increase in compound events is attributed to a shift towards storm surge weather patterns that also favour high precipitation. Our results demonstrate the importance of assessing compound flooding in a non-stationary framework and its linkages to weather and climate.

Nearly 40% of the US population resides in coastal counties[5]. Impacts of flooding in these usually low-lying, densely populated, and highly developed regions, can be devastating with wide-ranging social, economic and environmental consequences. Two distinct mechanisms—storm surges and heavy precipitation, either through direct runoff (pluvial) or increased river discharge (fluvial)—can lead to flooding in coastal areas. If they occur concurrently (or in close succession) the adverse consequences can be greatly exacerbated[1,2]. Recent compound events have resulted in substantial damages and loss of human life: for example, the Brisbane and Thailand Floods in 2011; hurricane Isaac and tropical storm Debby in 2012; typhoon Haiyan in 2013; and the series of winter storms in the UK in 2013/2014.

Compound flooding has often been assessed on a local scale[6–9], with regional studies limited to the UK (ref. 10), Netherlands[11] and Australia[12]. For the US, with many major coastal cities, including 17 port cities with population >1 million[13], the likelihood of the joint occurrence of the two natural hazard types has not been assessed so far. Here we investigate the spatial and temporal variability of the dependence between them using hourly storm surge data (tidal and mean sea level (MSL) influence removed) from 30 tide gauges (TGs; ref. 14) around the US and daily precipitation averages derived from stations[15] within 25 km of these TGs (Fig. 1a and Methods).

The complex interplay between storm surge and precipitation can lead to or exacerbate the impacts of flooding in coastal zones through multiple mechanisms. For mechanism (1), in estuarine regions, the joint occurrence of both may elevate water levels to a point where flooding is initiated or its impacts exacerbated. Mechanism (2) occurs when a destructive storm surge already causes widespread flooding, such that any significant rainfall on top of this—even if it is not an extreme event on its own—increases the flood depth and/or extent of the inundated area. Mechanism (3) occurs during a moderate storm surge which does not directly cause flooding, but is high enough to fully block or slow down gravity-fed storm water drainage, such that precipitation is more likely to cause flooding. Whether or not all of these mechanisms are relevant at a particular site strongly depends on the local setting. Here we capture all of the above-mentioned mechanisms by investigating the dependency between storm surge and precipitation for two distinct cases: in Case I we search for the highest annual storm surge, and then take the highest precipitation within a time range of ± 1 days of this event (covers mechanisms (1) and (2)); in Case II we search for the highest annual precipitation, and then take the highest storm surge within a time range of ± 1 days (covers mechanism (3)). We use Kendall's rank correlation coefficient τ (ref. 16) to reliably measure dependence between the two variables and use copula theory[17–19] to identify the appropriate dependence structure. The latter is important to include information on joint occurrences of extremes into flood risk analysis. Here we consider three extreme value copulas (Gumbel, Galambos and Hüsler-Reiss) and two from the Archimedean family (Frank, Clayton; the Gumbel copula belongs to both classes). We use tail dependence analysis[20] and compare observed and simulated data pairs by visual inspection (see Supplementary Fig. 1 for examples) to identify suitable copulas to model underlying dependence in the data (Methods). For Case I we find significant correlation, associated with a higher likelihood that compound flooding occurs, for virtually all sites along the Gulf and east coast, and one site in the southwest (Fig. 1b). In Case II significant dependency is confined to the Gulf and southeast coast, one site in the northeast, and three sites on the west coast (Fig. 1c). A sensitivity test using a 50 km radius around the TG sites to select precipitation stations reveals the same spatial pattern (Supplementary Fig. 2).

Variations in the dependency between rainfall and storm surge are also important because they alter the flood risk. We assess temporal changes by calculating τ for 50-year moving windows (shifted by one year each time step; Methods). The resulting time series from six sites with long overlapping records are shown in Fig. 2a–f. For San Francisco, results are shown for Case II, for the

[1]College of Marine Science, University of South Florida, 140 7th Avenue South, St Petersburg, Florida 33701, USA. [2]Research Centre Siegen, University of Siegen, Weidenauer Str 169, 57076 Siegen, Germany. [3]Civil and Environmental Engineering, Climate Change Institute & Mitchell Center for Sustainability Solutions, University of Maine, 5711 Boardman Hall, Orono, Maine 04469-5711, USA. [4]Research Institute for Water and Environment, University of Siegen, Paul-Bonatz Str 9-11, 57076 Siegen, Germany. *e-mail: thomas.wahl@uni-siegen.de

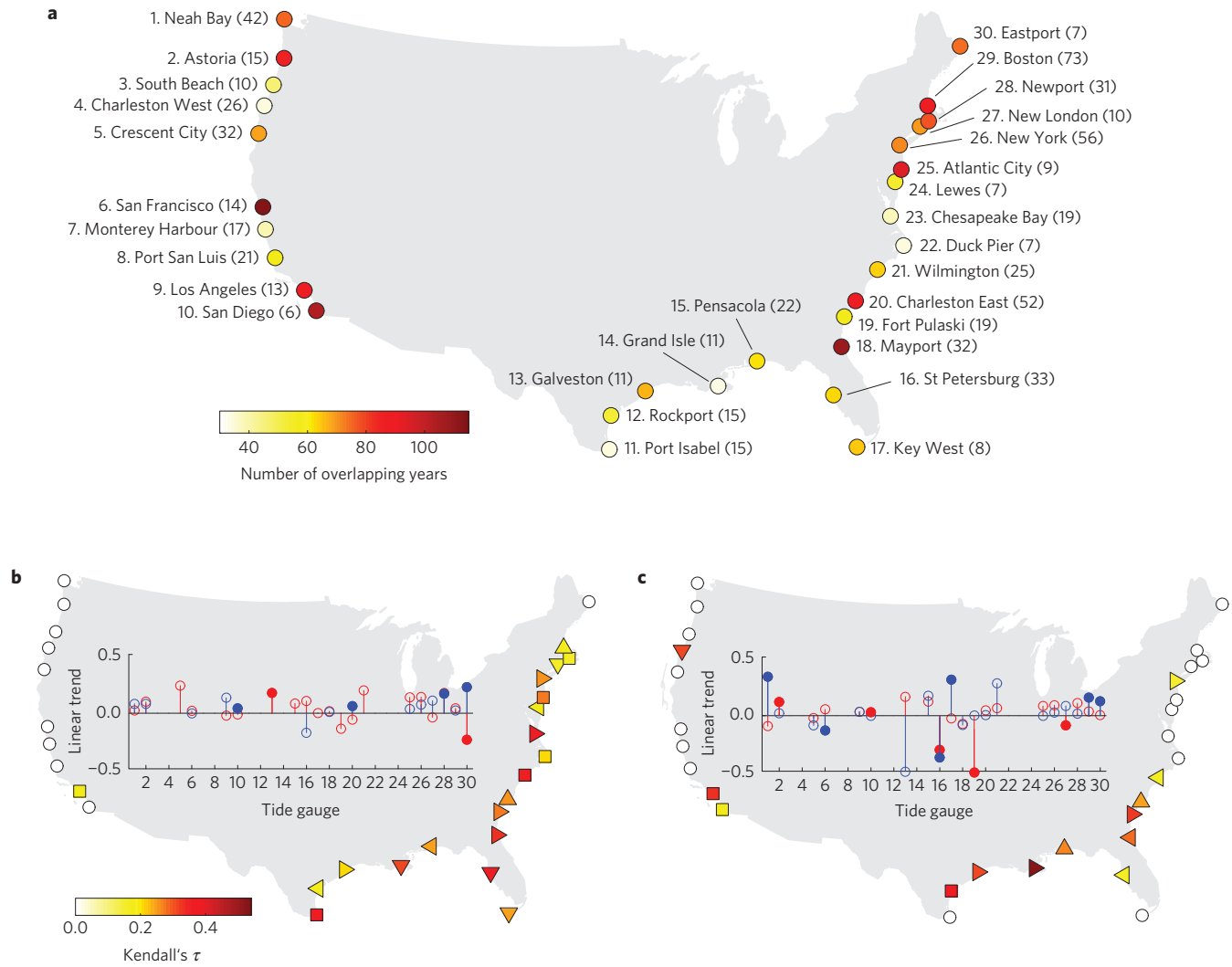

Figure 1 | Data sets and spatial variability of the dependency between storm surge and precipitation. a, TG locations; colour represents the number of overlapping years between storm surge and precipitation time series, numbers in brackets denote the number of precipitation stations in a radius of 25 km around the TGs. **b**,**c**, τ for Cases I (**b**) and II (**c**); markers denote the selected copula type (square is Frank; triangles pointing right, left, up and down are Gumbel, Clayton, Galambos and Hüsler-Reiss, respectively). Insets show linear trends for the storm surge (red; unit is cm yr^{-1}) and precipitation (blue; unit is mm yr^{-1}) time series for Cases I (**b**) and II (**c**) for all sites used in the non-stationary analysis (see text). Open circles denote insignificant correlations or trends (90% confidence).

other sites for Case I. At all six sites we find an increase in τ; in many instances it was insignificant (or even negative) in the first half of the twentieth century and became significant (90% confidence) over recent decades. The 90th percentiles of the natural variability (estimated with a resampling approach; Methods) have recently been exceeded at all six sites. The linear trends of the running τ time series for the six sites—and all other sites with at least 55 overlapping years of data and covering a period of at least 65 years (this criteria is fulfilled by 20 sites in total)—are depicted in Fig. 2g; for comparability, trends are calculated for the common period since 1948. Results are shown for Cases I and II for all sites where we find at least one significant positive trend (13 sites in total; see Methods for information on significance testing). This includes the major cities of San Francisco (TG 6), Los Angeles (TG 9), San Diego (TG 10), Houston (TG 13, Galveston), Tampa (TG 16, St Petersburg), NYC (TG 26) and Boston (TG 29). Comparing tail dependence coefficients (TDCs; ref. 20) derived from the first and second halves of the raw data sets (Methods and Supplementary Fig. 3) reveals that much of the observed increase in the overall dependency is due to higher incidence of joint events in the upper tail region, highly relevant for flood risk and design. Discrepancies between neighbouring sites may stem from regional or local effects, such as differences in the storm surge climate at multi-decadal timescales[21], or in actual precipitation amounts as a result of local factors. In some instances, we also find positive and negative trends at a single site (for example, Atlantic City); these may annul each other in terms of changes in the actual flood risk depending on the dominant flood mechanism in the area (generally Case I poses the greater risk for human lives in coastal regions[22]).

We analyse the data sets from NYC in more detail to attribute the observed changes in τ to synoptic-scale weather patterns driving compound or non-compound events. The pairs of ranks (rescaled by a factor of $1/(N+1)$, where N is the number of pairs), also known as pseudo-observations[23], shown in Fig. 3a,b reveal that most events from the past three to four decades lie close to the diagonal, indicating high correlation (especially in Case I; Fig. 3a), whereas many of the earlier ones are widely scattered; the same plots, but with real units, are shown in Supplementary Fig. 4. Events associated with tropical cyclones (filled squares) are identified using cyclone track information from the HURDAT (ref. 24) database (Methods)

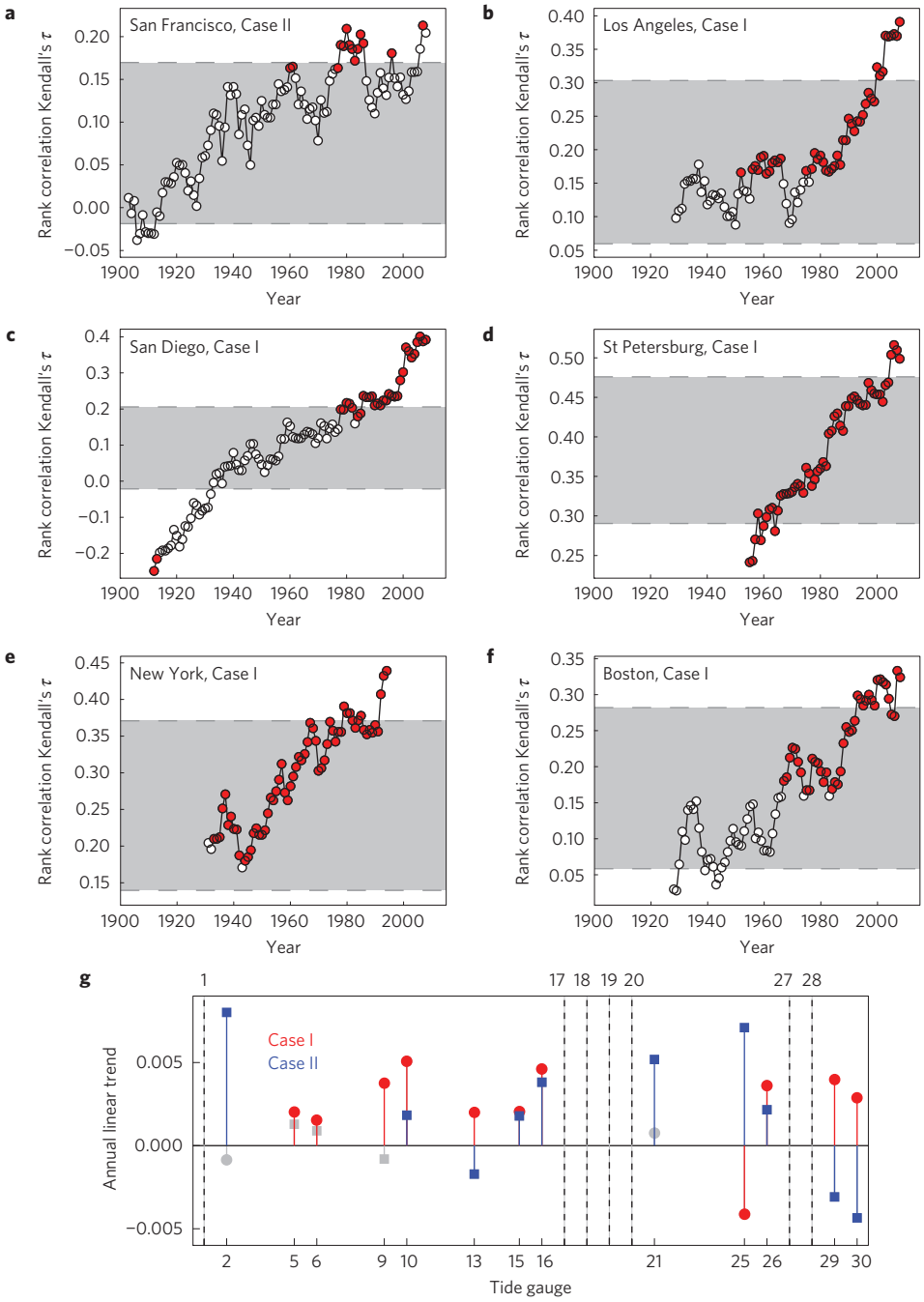

Figure 2 | Non-stationarity in the dependence between storm surge and precipitation. a–f, τ for 50-year running windows; filled circles denote significant correlation (90% confidence); grey shaded areas represent the range of natural variability (10% and 90% levels). **g**, Linear trends of running τ time series for the common period since 1948 for Cases I (red) and II (blue); results are shown only for sites with at least 55 overlapping years of data over a 65-year period. Dashed lines indicate sites that meet the record lengths criteria but do not exhibit significant trends.

and exhibit strong concordance between high storm surge and heavy precipitation. October 2012 hurricane Sandy (that is, the red square in the upper left of Fig. 3a) is an exception, stemming from a highly unusual impact angle, resulting in an extreme storm surge[25], whereas the amount of rainfall was small in the historical context for such an event.

We use maps of sea-level pressure (SLP) and winds from the Twentieth Century Reanalysis Project (20CR; ref. 26) to identify the prevailing synoptic weather situations that have caused selected storm surge events with high (that is, compound events) and low (that is, non-compound events) precipitation. The selected events from Cases I and II at the NYC TG are marked with grey squares (high storm surge and low precipitation) and grey circles (high storm surge and high precipitation) in Fig. 3a,b; events are selected here based on their ranks, the same plots with real units are shown in Supplementary Fig. 4. The SLP and wind composites depicted in Fig. 3c–f reveal that storm surges in NYC are accompanied by heavy precipitation when a high-pressure system stretches from Newfoundland south over the North Atlantic, from where moist air is transported into the low-pressure system causing the storm surge (Supplementary Fig. 5). When the high is confined to the mainland of North America, dry air (Supplementary Fig. 5) is transported to the site of interest, and no or only small amounts of precipitation occur with the storm surge. For TG Boston (located north of NYC),

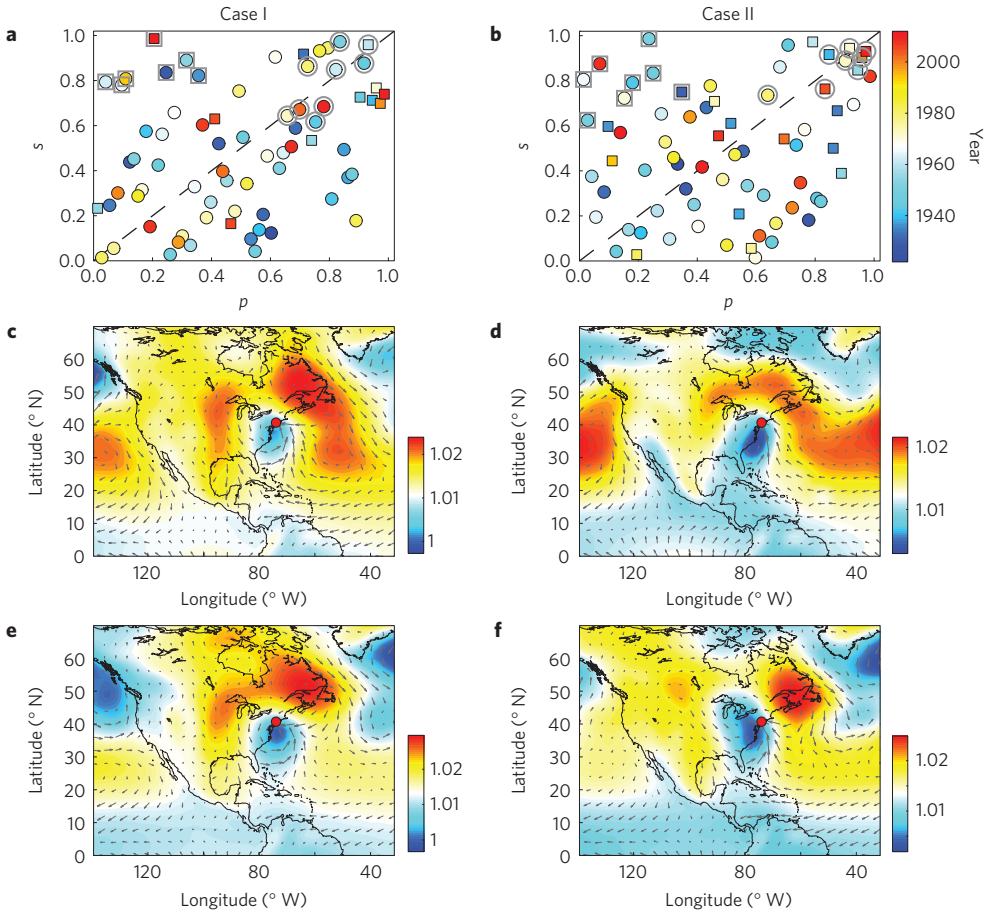

Figure 3 | Weather patterns associated with the increasing frequency of compound events in NYC. a,**b**, Rescaled pairs of ranks of storm surge (*s*) and precipitation (*p*); filled squares are tropical events; framed events were used for the composite plots; colour denotes the year of occurrence. **c**–**f**, Composite plots of SLP (unit is Pa × 10^5) and wind for events with high storm surge and high precipitation (**c**,**d**; circle frames in **a**,**b**) and high storm surge and low precipitation (**e**,**f**; square frames in **a**,**b**). Case I (**a**,**c**,**e**); Case II (**b**,**d**,**f**). The NYC TG location is shown by the red dot.

SLP, wind and precipitable water content (PWC) composites reveal similar spatial patterns for Case I (Supplementary Fig. 6) where the overall correlation is significant at both sites.

We use these results and calculate and compare the centred pattern correlation (CPC) coefficients[27] between the reference situations depicted in Fig. 3c–f and the SLP and wind fields of all individual Case I (CPC1) and Case II (CPC2) events at NYC (Methods). The difference between the summed (SLP + wind) CPC1 and CPC2 is used to attribute a respective event to one of the reference situations. When taking into account the entire time period for which data are available, the ratio between compound and non-compound events is 1.7 for Case I and 2.6 for Case II—that is, weather situations associated with compound events occur approximately twice as often. When we analyse the first and last 30-year periods separately the ratios increase from 2.7 to 5 in Case I and 2.8 to 3.5 in Case II. This independent approach confirms the results from the running τ and tail dependence analysis and highlights that weather patterns favouring high precipitation have dominated the storm surge climate in NYC over the past few decades.

To quantify the effect of observed changes in τ in NYC on joint return periods relevant to flood risk analyses (for example to define flood zones) and infrastructure design and adaptation, we perform a full multivariate statistical analysis (see Methods); we use the previously identified copula models (Fig. 1b,c) to capture the (non-stationary) dependence. We select a random extreme event combination comprised of 120 mm daily average rainfall and a storm surge of 115 cm. If the latter coincides with mean high water (66 cm above MSL at the Battery TG) it exceeds the height of the Manhattan sea wall (~125 to 175 cm above MSL; ref. 28). Similar conditions—that is, 118 mm daily rainfall and 114 cm storm surge—were observed at NYC in 1971 during tropical storm Doria. We find—for example—that if we use the smallest value of τ (as observed around the 1940s) the selected event had an 'AND' joint return period (JRP; that is, both variables exceed the respective threshold at the same time[29]) of ~105 years, close to the '100-year event' often used for design and adaptation planning. Using the highest value of τ (as observed recently) the JRP drops to ~42 years (that is, the likelihood that such an extreme compound event occurs has more than doubled). Falsely assuming independence between the two variables results in a JRP of ~245 years. Preserving the return period of 105 years under current conditions (that is, with the increased dependency) is associated with an increase of daily rainfall by 25% to 150 mm (assuming 115 cm storm surge) or an increase of the storm surge by more than 50% to 180 cm (assuming 120 mm rainfall). In the absence of significant long-term trends in time series of the marginal variables during the investigated time period (insets in Fig. 1b,c), our results indicate that the increase in the frequency of compound events stemmed from changes in the dependency (or joint distribution) alone. More research at local scales is needed to quantify the actual impacts associated with this, so as to ultimately include the information into optimized design guidelines and flood risk analyses, and thus define flood zones. This requires complex integrated modelling experiments (covering surface and drainage flows) including storm surge, rainfall and river

discharge (ideally at higher frequency than used in the present study) as coupled ocean–atmospheric processes[9], and should also consider the output of high-resolution climate models[9,30] to explore how joint dependence of extreme rainfall and storm surges may respond to future climate variability and change.

Methods

Methods and any associated references are available in the online version of the paper.

Received 24 February 2015; accepted 25 June 2015; published online 27 July 2015

References

1. Seneviratne S. *et al.* in *Managing the Risks of Extreme Events and Disasters to Advance Climate Change Adaptation* (eds Field, C. B. *et al.*) 109–230 (IPCC, Cambridge Univ. Press, 2012).
2. Leonard, M. *et al.* A compound event framework for understanding extreme impacts. *WIREs Clim. Change* **5,** 113–128 (2014).
3. Ezer, T. & Atkinson, L. P. Accelerated flooding along the U.S. East Coast: On the impact of sea level rise, tides, storms, the Gulf Stream and NAO. *Earth's Future* **2,** 362–382 (2014).
4. Sweet, W. V. & Park, J. From the extreme to the mean: Acceleration and tipping points of coastal inundation from sea level rise. *Earth's Future* **2,** 579–600 (2014).
5. *NOAA's State of The Coast* (NOAA, accessed 2 June 2014); http://stateofthecoast.noaa.gov/population
6. *Coincident Flooding in Queensland: Joint Probability and Dependence Methodologies* (Department of Science, Information Technology, Innovation and the Arts, Queensland Government, 2012).
7. Lian, J. J., Xu, K. & Ma, C. Joint impact of rainfall and tidal level on flood risk in a coastal city with a complex river network: A case study of Fuzhou City, China. *Hydrol. Earth Syst. Sci.* **17,** 679–689 (2013).
8. Chen, W.-B. & Liu, W.-C. Modeling flood inundation induced by river flow and storm surges over a river basin. *Water* **6,** 3182–3199 (2014).
9. Van den Hurk, B., van Meijgaard, E., deValk, P., van Heeringen, K.-J. & Goijer, J. Analysis of a compounding surge and precipitation event in the Netherlands. *Environ. Res. Lett.* **10,** 035001 (2015).
10. Svensson, C. & Jones, D. A. Dependence between sea surge, river flow and precipitation in south and west Britain. *Hydrol. Earth Syst. Sci.* **8,** 973–992 (2004).
11. Kew, S. F., Selten, F. M., Lenderink, G. & Hazeleger, W. The simultaneous occurrence of surge and discharge extremes for the Rhine delta. *Nature Hazard Earth Sys.* **13,** 2017–2029 (2013).
12. Zheng, F., Westra, S. & Sisson, S. A. Quantifying the dependence between extreme rainfall and storm surge in the coastal zone. *J. Hydrol.* **505,** 172–187 (2013).
13. Hanson, S. *et al.* A global ranking of port cities with high exposure to climate extremes. *Climatic Change* **104,** 89–111 (2011).
14. *Joint Archive for Sea Level (JASL) Research Quality Data Set (RQDS)* (University of Hawaii Sea Level Center, accessed 17 November 2013); http://uhslc.soest.hawaii.edu/data/download/rq
15. *NOAA Precipitation Data* (National Climatic Data Center, accessed 22 January 2014); http://gis.ncdc.noaa.gov/map/viewer/#app=cdo&cfg=cdo&theme=precip&layers=000111
16. Kendall, M. A new measure of rank correlation. *Biometrika* **30,** 81–89 (1938).
17. Nelsen, R. B. *Lecture Notes in Statistics* 2nd edn, Vol. 139 (Springer, 2006).
18. Grimaldi, S. & Serinaldi, F. Asymmetric copula in multivariate flood frequency analysis. *Adv. Water Resour.* **29,** 1115–1167 (2006).
19. De Michele, C. & Salvadori, G. A Generalized Pareto intensity-duration model of storm rainfall exploiting 2-copulas. *J. Geophys. Res.* **108,** 4067 (2003).
20. Schmidt, R. & Stadmüller, U. Nonparametric estimation of tail dependence. *Scand. J. Stat.* **33,** 307–335 (2006).
21. Wahl, T. & Chambers, D. P. Evidence for multidecadal variability in US extreme sea level records. *J. Geophys. Res.* **120,** 1527–1544 (2015).
22. Jonkman, S. N., Vrijling, J. K. & Vrouwenvelder, A. C. W. M. Methods for the estimation of loss of life due to floods: A literature review and a proposal for a new method. *Nature Hazards* **46,** 353–389 (2008).
23. Kojadinovic, I. & Yan, J. Modeling multivariate distributions with continuous margins using the copula R package. *J. Stat. Softw.* **34,** 1–20 (2010).
24. *HURDAT Best Track Data* (NOAA Hurricane Research Division of AOML, 2014); http://www.aoml.noaa.gov/hrd/hurdat/tracks1949to2011_epa.html
25. Hall, T. M. & Sobel, A. H. On the impact angle of Hurricane Sandy's New Jersey landfall. *Geophys. Res. Lett.* **40,** 2312–2315 (2013).
26. Compo, G. P. *et al.* The twentieth century reanalysis project. *Q. J. R. Meteorol. Soc.* **137,** 1–28 (2011).
27. Santer, B. D., Wigley, T. M. L. & Jones, P. D. Correlation methods in fingerprint detection studies. *Clim. Dynam.* **8,** 265–276 (1993).
28. Colle, B. A. *et al.* New York City's vulnerability to coastal flooding. *Bull. Amer. Meteorol. Soc.* **89,** 829–841 (2008).
29. Gräler, B. *et al.* Multivariate return periods in hydrology: A critical and practical review focusing on synthetic design hydrograph estimation. *Hydrol. Earth Syst. Sci.* **17,** 1281–1296 (2013).
30. Kendon, E. J. *et al.* Heavier summer downpours with climate change revealed by weather forecast resolution model. *Nature Clim. Change* **4,** 570–576 (2014).

Acknowledgements

T.W. was supported by a fellowship within the postdoctoral programme of the German Academic Exchange Service (DAAD). I. D. Haigh assisted in editing the manuscript.

Author contributions

T.W. conceived the idea of the study, performed the analyses and wrote the paper; J.B. assisted in writing MATLAB code, participated in technical discussions and co-wrote the paper; S.J. provided guidance on selecting the precipitation data, assisted in performing the statistical analyses and co-wrote the paper; S.D.M. and M.E.L. participated in technical discussions at an early stage when the idea for the study evolved and co-wrote the paper.

Additional information

Supplementary information is available in the online version of the paper. Reprints and permissions information is available online at www.nature.com/reprints. Correspondence and requests for materials should be addressed to T.W.

Competing financial interests

The authors declare no competing financial interests.

Methods

Data selection and processing. Hourly sea-level records[14] from 30 tide gauges (TGs) with at least 30 years of data between 1900 and 2012 are used for the study. If two or more TGs are located within 55 km, only the longer record is used, to avoid the same precipitation stations being allocated to more than one TG. The data at Mayport started in 1928 and ended in 2000, and was merged with Fernandina Beach (located only 31 km north of Mayport) TG data for the periods from 1897 to 1928 and 2001 to 2012. For the overlapping period (1985 to 2000) the correlation between the two raw data sets is 0.99. After this correction all records end in December 2012. The MATLAB T_Tide package[31] is used for a year-by-year harmonic tidal analysis (with 67 constituents), which also effectively removes the MSL influence (including the seasonal MSL cycle). Years with less than 75% of data were omitted from the analysis (this affects less than 3% of the overall data). A visual inspection of the storm surge time series (tidal signal removed) revealed obvious outliers at several TGs. For Gulf and east coast stations these could be related to strong hurricanes or extratropical storms; on the west coast tsunamis were responsible for the highest water levels at several sites. Such events are driven by different mechanisms and often triggered thousands of kilometres away. Therefore we should not assume any relationship with rainfall events. We removed the following days from the records of all TGs located on the west coast: 23 May 1960 (Great Chilean Earthquake), 28 March 1964 (Great Alaskan Earthquake), 11/12 March 2011 (2011 Tōhoku earthquake in Japan). We note that measured water levels were possibly affected by tsunamis at other times throughout the past century, but did not always result in large sea-level anomalies at the sites of interest, and can therefore be neglected for the purpose of the present study.

Cumulative daily precipitation records[15] from stations in a radius of 25 km around the TG sites are used. There are two exceptions to this rule: for Grand Isle we select stations in a radius of 50 km, as the TG is located offshore and there is only one precipitation station within 25 km, which covers a period much shorter than the TG record; for Neah Bay we use a radius of 35 km, as there are only few precipitation stations within 25 km of the TG and the time period covered by them is shorter than the TG record. All precipitation records allocated to a TG are averaged into a single time series and compared to the storm surge records. Generally, the precipitation time series are longer and more complete than the TG records; the entire precipitation time series are used to identify the overlapping periods which are then considered for the dependence study. A sensitivity test using a 50 km radius instead of 25 km reveals that the τ values derived for the 30 sites are not considerably affected by this definition (Supplementary Fig. 2). For Australia, significant correlation between precipitation and storm surge was found for much larger spatial distances (up to 1,000 km), but decreases further away from the coast[12].

The significance of the linear trends of the raw data sets—that is, the annual maximum and coincident event time series (insets in Fig. 1b,c)—is tested with a modified Mann–Kendall Test for autocorrelated data[32].

Dependence measure and modelling. Dependence between storm surge and precipitation is measured through Kendall's rank correlation coefficient τ (ref. 16) (as opposed to Pearson's correlation coefficient, which captures only linear relationships). Storm surges sometimes occurred without precipitation, and this leads to ties (several zero values) in the Case I data sets. These ties are broken as suggested in ref. 23, by assigning ranks randomly. This may have a small effect on the rank correlation when the number of ties is large; therefore we repeat the procedure 100 times and calculate the average rank correlation. Copula parameters are derived with the maximum pseudo-likelihood estimator[23]. Copula models capable of simulating the prevailing dependence structures are selected by visually inspecting the observed and simulated (1,000 data pairs) pairs of ranks (or pseudo-observation clouds; see Supplementary Fig. 1 for examples) and using tail dependence analysis by comparing non-parametric TDCs (ref. 20) above a threshold of 0.6, derived from observed and simulated rank pairs.

Temporal changes in the overall rank correlation and tail dependency. The rank correlation is calculated for 50-year moving windows (shifted by one year each time step). In each window we required at least 30 data pairs to assure robust estimates of τ. From this it follows, to be consistent, that at the beginning (end) of the time series, τ is calculated from the first (last) 30 data pairs if all values are available (that is, we shift the 50-year windows beyond the edges of the available time series and calculate τ values as long as 30 data pairs are available).

The significance of the temporal changes in τ is assessed in two ways. First, for six selected sites and cases (among Cases I and II) the range of the natural variability (10% and 90% levels) of the rank correlation is derived by resampling τ (from 50 data pairs) 10,000 times (Fig. 2a–f). Second, we calculate linear trends of the running τ time series for the common period since 1948 and test the significance with a similar resampling approach: the ranks of the raw data sets are randomly rearranged (1,000 times) and the running τ time series and linear trends are recalculated; the 30% and 70% quantiles are used to identify significant trends. Here we chose these relatively low levels because the number of degrees of freedom is small as a result of the running window approach, the linear model might not be ideal if τ increased rapidly recently after having been relatively stable before (for example, Fig. 2b), and most importantly the results from the multivariate statistical analysis reveal that the observed changes in τ—even if the trends are not significant at high confidence levels (for example, 90%)—greatly affect joint return periods; the estimated slopes at sites with significant trends range from ~0.002 to ~0.008, which equals an increase in τ of 0.1 to 0.4 over a 50-year period (or 0.2 to 0.8 over 100 years).

TDCs for the first and second halves of the raw data sets and above a threshold of 0.6 are compared to investigate whether similar changes as found in the overall rank correlation are also evident in the upper tails (Supplementary Fig. 3).

Tropical/extratropical and compound/non-compound events in NYC. We use the HURDAT database[24] to distinguish between tropical and extratropical storm surge events that were recorded at the Battery TG in NYC. When the time stamp of the day of a particular event occurs in the HURDAT database and the respective storm entered the region east of 70° W longitude and north of 30° N latitude at some point in its life we assume that it was a tropical event, otherwise it is flagged as an extratropical event.

We identify compound and non-compound events based on the empirical non-exceedance probabilities of storm surge (s) and precipitation (p). The events with grey squares in Figs. 3a and 3b fulfil the criteria $s > 0.6$, $p < 0.4$ and $p > s + 0.4$ (that is, s is high, p is small, and the events lie far above the diagonal), events with grey circles satisfy $s > 0.6$, $p > 0.6$, $p < s + 0.15$ and $p > s - 0.15$ (that is, s and p are high and events lie close to the diagonal).

Weather patterns associated with compound/non-compound events in NYC. SLP, PWC and wind fields from the 20CR (ref. 26) and the days when the selected compound/non-compound events (see previous paragraph) occurred are averaged into composites, representing reference synoptic-scale weather situations favouring the occurrence of storm surges with much (Fig. 3c,d) or little (Fig. 3e,f) precipitation; the PWC composites are shown in Supplementary Fig. 5. We apply the concept of centred pattern correlation (CPC; ref. 27) as a widely used pattern similarity statistic in climate studies to correlate, for each spatial point, SLP and wind fields from all 'event days' in NYC with the composites used as reference situations (shown in Fig. 3c–f). We focus on the area between 70° to 40° W and 20° to 60° N, as the reference composites reveal that the prevailing SLP and wind situation in this area determines whether a storm surge is accompanied by large or small amounts of precipitation. The summed CPC coefficients (SLP + winds) with the low-precipitation reference situation (CPC2; Fig. 3e,f) are subtracted from the summed CPC coefficients with the high-precipitation reference situation (CPC1; Fig. 3c,d); if the difference is >0.5 the respective event is flagged as a compound event, if it is <−0.5 the event is flagged as a non-compound event, and if it is in between it is not allocated to either of the two. We then calculate ratios between compound and non-compound events from the Case I and II data sets for the entire records and for the first and last 30-year periods separately.

Multivariate statistical analysis for NYC. We perform a full multivariate statistical analysis for the data set from NYC to demonstrate the effect of a changing rank correlation (that is, changes in the joint distribution) on multivariate return periods of variables relevant to flood risk analysis and infrastructure design/adaptation. The marginal distributions for Cases I and II were selected from a pool of five distributions commonly used in hydrology and (coastal) engineering, namely the LogNormal distribution, normal distribution, exponential distribution, Weibull distribution, and the generalized extreme value (GEV) distribution. A goodness-of-fit (GoF) test comparing the empirical and theoretical non-exceedance probabilities using the root mean squared error was applied to identify the distributions fitting best to the underlying data sets; distribution parameters were estimated with the maximum likelihood method. We use two Gumbel copulas—identified with the GoF test(s) employed here—to analyse the Case I and Case II data sets separately. To quantify the effect of changes in the dependency, the analysis is performed with the highest and lowest values of the running τ time series in Fig. 2e. The relevant 'AND' joint return periods[29] are calculated for a selected compound event.

References

31. Pawlowicz, R., Beardsley, B. & Lentz, S. Classical tidal harmonic analysis including error estimates in MATLAB using T_TIDE. *Comput. Geosci.* **28,** 929–937 (2002).
32. Hamed, K. H. & Rao, A. R. A modified Mann–Kendall trend test for autocorrelated data. *J. Hydrol.* **204,** 182–196 (1998).